ORGANOMETALLICS

Article

Cite This: *Organometallics* 2019, 38, 1502−1515

pubs.acs.org/Organometallics

Oxidative Additions to Ti(IV) in [(dadi)$^{4-}$]Ti^{IV}(THF) Involve Carbon−Carbon Bond Formation and Redox-Noninnocent Behavior

Spencer P. Heins,[†] Bufan Zhang,[†] Samantha N. MacMillan,[†] Thomas R. Cundari,[‡] and Peter T. Wolczanski*[,†]

[†]Department of Chemistry & Chemical Biology, Baker Laboratory, Cornell University, Ithaca, New York 14853, United States

[‡]Department of Chemistry, CASCaM, University of North Texas, Denton, Texas 76201, United States

Supporting Information

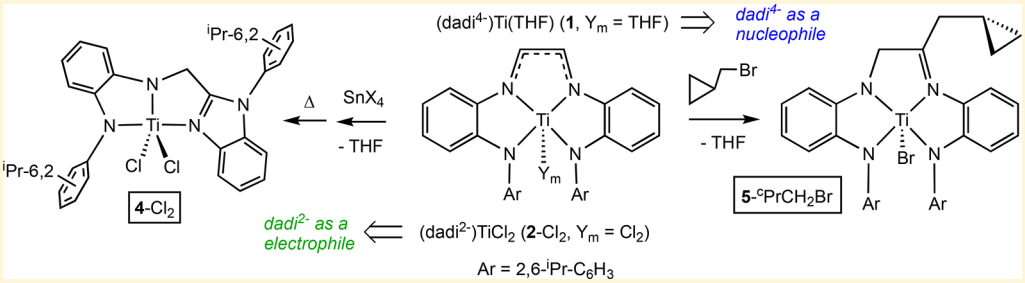

ABSTRACT: An attempt at transferring the imide of (dadi)Ti=NAd (**2**=NAd, dadi^{2-}, dadi^{n} = [{−CH=N(1,2-C_6H_4)N(2,6-$^{i}Pr_2$-C_6H_3)}$_2$]^{n})to C_2H_4 led instead to low yields of *trans*-C_6H_4-{1,2-(*N*,2-*N*(2,6-$^{i}Pr_2$-C_6H_3)-C_6H_4)$_2$Ti-NHAd}$_2$ (**3**), a product that features four new C−C bonds to two new carbons. Mechanistic evaluation of its formation led to oxidative addition studies of SnX_4 (X = Cl, Br, I) and RX to (dadi)Ti(THF) (**1**-THF, dadi^{4-}), in which the oxidation occurs at the dadi ligand. Products include (dadi)TiX_2 (**2**-X_2, X = Cl, Br, I) and the imine-triamide (R-ita)TiX (**5**-RX, R = Me, Bn; X = Cl, Br; R-ita = [{−CH_2N(1,2-C_6H_4)N(2,6-$^{i}Pr_2$-C_6H_3)}{CR=N(1,2-C_6H_4)N(2,6-$^{i}Pr_2$-C_6H_3)}]). Studies of the RX additions, including implementation of radical clocks, pointed toward concerted process(es). Rearrangements of **2**-X_2 and **2**=NAd revealed a new tridentate benzimidazole diamide chelate (bida) structurally characterized in (bida)$TiCl_2$ (**4**-Cl_2) and (bida)Ti=NAd ($OPMe_2Ph$) (**6**). The nature of various products suggests that the (dadi^{n})Ti core can act as a nucleophile (*n* = 4), electrophile (*n* = 2), or as a radical center (*n* = 3) under certain conditions.

INTRODUCTION

Carbon−carbon bond formation is often a consequence of redox noninnocence (RNI) that induces radical character in certain ligands.[1−5] In many cases, a relatively simple coupling of carbon radicals occurs to form a single new bond, but sometimes the reactivity can be complicated. Figure 1 illustrates some unusual C−C bond forming events discovered in these laboratories.[6−13] In **A**, the Ti(III) complex, (smif)-{Li(smif−smif)}Ti, was shown to contain one C−C bond derived from coupling of smif (smif = 1,3-di(2-pyridyl)-2-azaallyl) ligands that were reduced during the course of its synthesis. One mode of its decomposition generated dimer [(smif^{2-})Ti^{III}]$_2$(μ-κ^3,κ^3-*N*,*N*(py)$_2$-smif,smif), which contained two new C−C bonds that can be construed as arising from coupling of a singlet diradical, or alternatively, a nucleophile/electrophile coupling.[6] In **B**, the *in situ* generation of dark green (smif)Fe{N($SiMe_3$)$_2$} led to the isolation of its orange dimer, [{(Me_3Si)$_2$N}Fe]$_2$(μ-κ^3,κ^3-*N*,py$_2$-smif,smif), via the equilibrium shown. The two new C−C bonds are formed reversibly, as dissolution of the dimer regenerates the dark green solution, and UV−vis absorptions are characteristic of a metal bound smif anion.[7]

While **A** and **B** provide relatively simple examples of dimerization due to dual C−C bonds, **C** illustrates a complicated product formed during a degradation of the dianionic Ni(II) complex, [{Me_2C(CH_2NCH-py)$_2$}-Ni]$^{2-}$[K^{+}(THF)$_2$]$_2$, upon attempts to crystallize it using crypt-2.2.2.[10] Five-membered eneamide rings are generated from coupling of 1,3-di(2-pyridyl)-2-azaallyl components of the original chelate concomitant with dehydrogenation. Perhaps the most intriguing example is found in **D**, where attempts at chelation of M(II) diamides with Me_2C(CH=NCH_2−py)$_2$ led to the creation of 3 new C−C bonds, a metal−metal bond, and six new stereocenters as {Me_2C-(CHNCH-py)$_2$}M_2 (M = Cr, Co, Ni) were formed.[11,12]

Recently, these laboratories have focused on studies involving the diamide-diamin(d)e dadi^{n} ligand (dadi^{n} = [{−CH=N(1,2-C_6H_4)N(2,6-$^{i}Pr_2$-C_6H_3)}$_2$]^{n}), a tetradentate species that has at least five potential redox states.[14−16] The sterically hindered dadi^{n} ligand is not prone to radical coupling, as it exists mostly in closed-shell, di- and tetra-anionic (*n* = 2−, 4−) forms. In studying (dadi)Ti=NAd for potential nitrene

Received: December 24, 2018
Published: March 6, 2019

DOI: 10.1021/acs.organomet.8b00930
Organometallics 2019, 38, 1502−1515

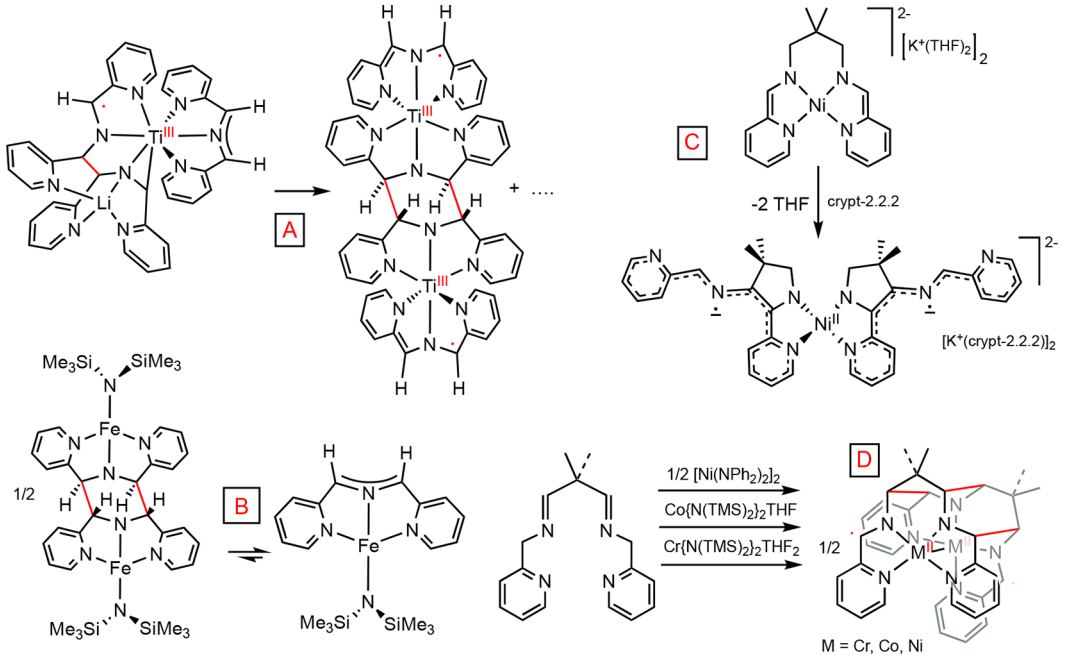

Figure 1. Examples of multiple C−C bond formation from first row transition elements.

Scheme 1. Discovery of *trans*-C_6H_4-{1,2-(*N*,2-*N*(2,6-^{i}Pr$_2$-C_6H_3)-C_6H_4)$_2$Ti-NHAd}$_2$ (3) and Key NMR Spectral Features[a]

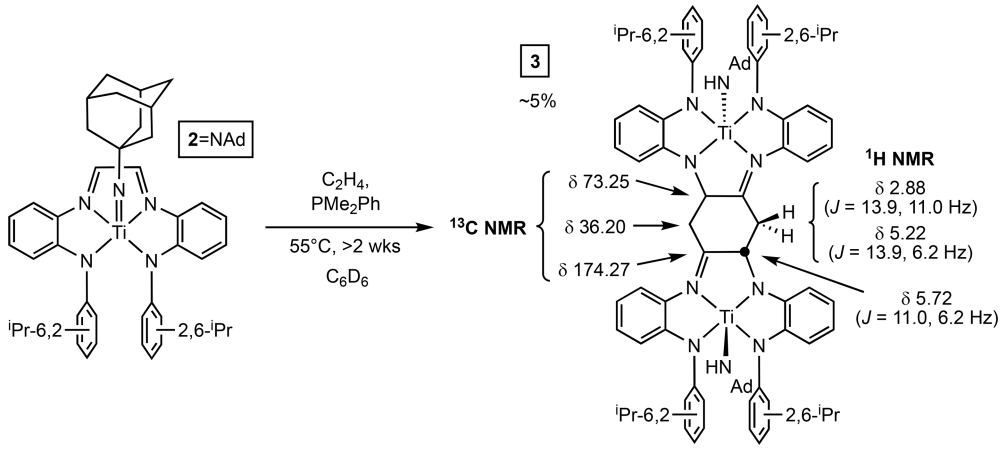

[a]The methine hydrogen at δ 5.72 was correlated to the δ 73.25 ^{13}C shift via an HSQC experiment, and the CH_2−CH ring spin system was determined via a gCOSY experiment.

transfer reactivity, a low-yielding reaction was found in which the complex incorporated two additional $-CH_2-$ groups via the formation of four new C−C bonds. When the reaction proved to be sporadic, mechanistic evaluation prompted a study of RX additions to (dadi^{4-})Ti^{IV}(THF) (**1**) and related chemistry. Herein are reported the oxidative addition of various RX and X_2 equivalents to Ti(IV), and accompanying reactivity relevant to C−C bond formation due to RNI.[17−20]

RESULTS AND DISCUSSION

Unusual Dimerization via C−C Bond Formation. *Discovery of trans-C_6H_4-{1,2-(N,2-N(2,6-^{i}Pr$_2$-C_6H_3)-C_6H_4)$_2$Ti-NHAd (**3**).* The adamantyl imide, (dadi)Ti═NAd (**2**═NAd; *d*(Ti−N) = 1.702(5) Å), synthesized from (dadi)Ti(THF) (**1**-THF) and AdN_3 (Ad = adamantyl),[15,16] seemed a logical candidate for nitrene transfer chemistry. Studies showed that **2**═NAd was a catalyst for the carbonylation of AdN_3 to AdNCO and N_2,[15] and ethylene was chosen as a plausible substrate for aziridine formation.

As Scheme 1 illustrates, **2**═NAd was treated with ethylene in the presence of PMe_2Ph, which was added to capture (dadi)Ti (**1**) as the phosphine adduct, (dadi)TiPMe_2Ph (**1**-PMe_2Ph).[15] No evidence of nitrene transfer was seen, even when the temperature was elevated to 55 °C over a period of ∼5 weeks. An NMR spectrum of the reaction residue revealed a multitude of resonances, and brown microcrystals were found deposited on the sides of the reaction vessel. The relative insolubility of the harvested material in common solvents hampered initial spectral analysis, and an X-ray structure determination was undertaken. The product was determined to be *trans*-C_6H_4-{1,2-(*N*,2-*N*(2,6-^{i}Pr$_2$-C_6H_3)-C_6H_4)$_2$Ti-NHAd}$_2$ (**3**), an unusual dimer in which two additional methylene units are found in addition to the atoms present in **2**═NAd, and the adamanyl imide has been converted to an amide.

DOI: 10.1021/acs.organomet.8b00930
Organometallics 2019, 38, 1502−1515

*X-ray Structure of trans-C_6H_4-{1,2-(N,2-N(2,6-^{i}Pr$_2$-C_6H_3)-C_6H_4)$_2$Ti-NHAd}$_2$ (**3**).* Figure 2 illustrates a molecular view of

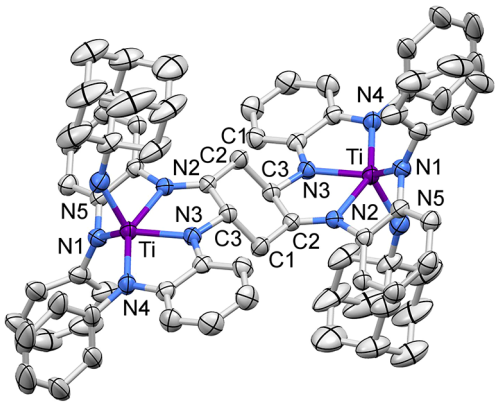

Figure 2. Molecular view of *trans*-C_6H_4-{1,2-(*N*,2-*N*(2,6-^{i}Pr$_2$-C_6H_3)-C_6H_4)$_2$Ti-NHAd}$_2$ (**3**). Selected distances (Å) and angles (deg): Ti–N1,1.995(2); Ti–N2, 2.142(2); Ti–N3, 1.980(2); Ti–N4, 2.006(2); TiN5, 1.886(3); C2N2, 1.283(3); C3N3, 1.441(3); N5–Ti–N1, 104.22(11)°; N5–Ti–N2, 90.47(10); N5–Ti–N3, 112.75(11); N5–Ti–N4, 110.03(11)°; N1–Ti–N2, 76.59(9)°; N1–Ti–N3, 131.82(10); N1–Ti–N4, 116.83(10); N2–Ti–N3, 73.41(8); N2–Ti–N4, 150.05(9); N3–Ti–N4, 78.47(9); Ti–N5–C, 140.6(2).

trans-C_6H_4-{1,2-(*N*,2-*N*(2,6-^{i}Pr$_2$-C_6H_3)-C_6H_4)$_2$Ti-NHAd}$_2$ (**3**), which sits on an inversion center. Bridging the two titanium centers is a six-membered ring with opposing imine (d(C═N) = 1.283(3) Å) and amide (d(C–N) = 1.441(3) Å) components,[21] each in a *trans*-arrangement. The adamantyl amide is clearly delineated by a d(Ti–N5) of 1.886(3) Å, and a Ti–N5–C angle of 140.6(2)°. Likewise, the imine nitrogen of the trianionic chelate is differentiated (d(Ti–N2) = 2.142(2) Å) from the three amides (d(Ti–N1) = 1.995(2), d(Ti–N3) = 1.980(2) Å, d(Ti–N4) = 2.006(2) Å). The titanium core is a distorted square pyramid, with the AdNH group at the apical position: ∠N5–Ti–N1 = 104.22(11)°, ∠N5–Ti–N2 = 90.47(10)°, ∠N5–Ti–N3 = 112.75(11)°, ∠N5–Ti–N4 = 110.03(11)°. Angles among the basal nitrogens range from the bite angle of 73.41(8)°, assessed to ∠N2–Ti–N3, to bite angles of ∠N1–Ti–N2 = 76.59(9)° and ∠N3–Ti–N4 = 78.47(9)° corresponding to the 1,2-aryl-substituted nitrogens, to the expected wide ∠N1–Ti–N4 = 116.83(10)° accorded the diamide portion derived from the original dadi ligand. The *trans*-basal angles are ∠N1–Ti–N3 = 131.82(10)° and ∠N2–Ti–N4 = 150.05(9)°, leading to an Addison parameter of 0.30.[22]

Labeled Ethylene Studies. The methylene groups incorporated in *trans*-C_6H_4-{1,2-(*N*,2-*N*(2,6-^{i}Pr$_2$-C_6H_3)-C_6H_4)$_2$Ti-NHAd}$_2$ (**3**) appeared to derive from ethylene, and an 800 MHz ^{1}H NMR spectrum was acquired to overcome solubility issues and identify the resonances of the $-CH_2-$ groups. Diastereotopic protons of the methylene group resonated as doublets of doublets at δ 2.88 and δ 5.22, coupling to each other (13.9 Hz) and to the adjacent methine (J = 11.0 Hz, J = 6.2 Hz). Identification of the resonances was achieved via correlation spectroscopy (see the Supporting Information and Scheme 1), which was used to find the methine, methylene, and imine carbon chemical shifts at δ 73.25, 36.20, and 174.27, respectively. Sonication of the crystals and eventual dissolution enabled lower field NMR spectroscopic instruments to assay subsequent experiments, once the spectral shifts were assigned.

Individual experiments similar to Scheme 1 were conducted with $^{13}C_2H_4$ and C_2D_4, using the same batch of PMe_2Ph, and brown crystals developed over the course of several weeks. These were separated, collected, and subjected to NMR spectroscopic analysis, but no incorporation of ^{13}C or D was detected in either experiment. It was evident that the $-CH_2-$ units were derived from something besides ethylene, whose concentration (2 equiv, 1 or 5 atm) had no impact on whether dimer **3** was observed. Formation of *trans*-C_6H_4-{1,2-(*N*,2-*N*(2,6-^{i}Pr$_2$-C_6H_3)-C_6H_4)$_2$Ti-NHAd}$_2$ (**3**) was also somewhat sporadic, and the addition of 1,4-cyclohexadiene inhibited formation of **3**. Furthermore, the generation of **3** via PMe_2Ph proved to be dependent on the phosphine source (see the Supporting Information). As attention turned to the phosphine as the source of the $-CH_2-$ units, the generation of **3** through a radical path seemed likely. A fundamental study of oxidative addition to (dadi)Ti(THF) (**1**-THF) was then undertaken to assay general oxidative processes for radical activity.

Nature of (dadi)Ti(THF) (1-THF). Previous work has shown that oxidation of (dadi^{4-})Ti(THF) (**1**-THF) with RN_3 and N_2O formed (dadi^{2-})Ti^{IV}=Y (**2**═Y; Y = NR (R = Ad, $SiMe_3$), O),[15,16] respectively, as the chelate was oxidized. Figure 3 illustrates the three plausible redox states of (dadi)^n: (1) (dadi)$^{4-}$ in (dadi)TiL (**1**-L), which renders the NCHCHN backbone nucleophilic by its eneamide character; (2) (dadi)$^{2-}$ in **2**═Y, in which the diimine backbone is electrophilic; and (3) (dadi)$^{3-}$ in (dadi)Ti (**1**) which is radical in nature.

Since (dadi)Ti (**1**) cannot be observed, calculations were employed to determine its nature. CAS(12,12)[23]/SBKJC-(d))[24] calculations were performed at the DFT-optimized geometry of a truncated ^{1}Ti(dadi′) model. Via these MCSCF calculations, the singlet ground state was revealed to have significant biradical character. The two natural orbitals shown in Figure 4 have occupancies far removed from integer values and are delocalized across Ti and the N_2C_2 core of the dadi′ ligand: (Ti dπ+π_{NCCN})$^{1.56e-}$ (Ti dπ–π_{NCCN})$^{0.46e-}$. The former, shown in Figure 4a, is 53% Ti via a Mulliken analysis, while the

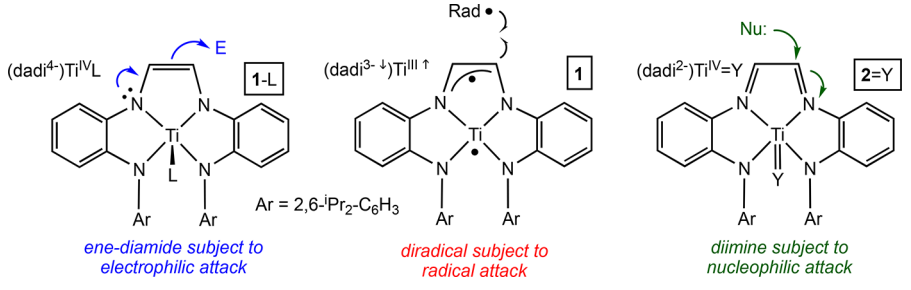

Figure 3. (dadi)Ti(L/Y)$_m$ structures featuring different redox states of dadi^n.

DOI: 10.1021/acs.organomet.8b00930
Organometallics 2019, 38, 1502–1515

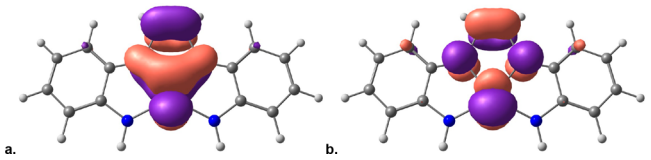

Figure 4. Natural orbitals from a CAS(12,12)/SBKJC(d) calculation at the DFT-optimized ground state of singlet $(d^1\text{-}Ti^{III})^{\uparrow}(dadi^{3-})^{\downarrow}$. Isovalue = 0.04.

latter natural orbital, shown in Figure 4b, is 50% Ti in character. The delocalization and significant correlation between these two orbitals supports a ground electronic state with antiferromagnetically coupled (AF) character (i.e., $(dadi^{3-})^{\downarrow}Ti^{III\uparrow}$) where the dadi radical trianion couples to d^1 Ti(III). Oxidative additions to $(dadi^{4-})Ti^{IV}$(THF) (**1**-THF) may indicate radical, concerted or polar character, but since the reactions can take place with THF bound or unbound, predictions of the number of dadi or Ti electrons removed are somewhat subject to interpretation.

Additions of X_2 (X = halide) Equivalents to (dadi)Ti-(THF) (1-THF). *(dadi)$_2$TiX$_2$ (**2**-X$_2$; X = Cl, Br, I).* Additions of X_2 to (dadi)Ti(THF) (**1**-THF) led to mixtures of products, presumably due to competitive halogenation sites on or around the metal or nonspecific radical reactivity; hence, typical X atom sources were sought as alternatives. The first successful alternate route used *N*-chlorosuccinamide, which generated a green product, formulated as (dadi)TiCl$_2$ (**2**-Cl$_2$), as shown in eq 1.

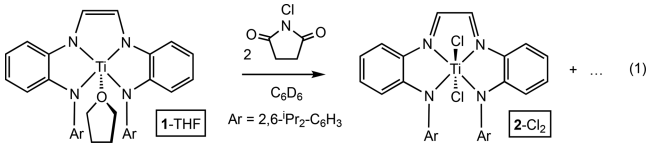

The dichloride possesses C_{2v} symmetry according to ^{1}H NMR spectroscopy, as the spectrum indicated the presence of two mirror planes. Byproducts from the reaction proved difficult to separate, and since the yield was modest (40%), additional routes were sought. Once **2**-Cl$_2$ was identified, it was also noticed in the treatment of **1**-THF with CCl_4, but deleterious byproducts again posed a separation problem. Hexachloropropene also served as a chlorine atom source when added to **1**-THF in the presence of 10 mol % azo-*bis*-isobutyronitrile (AIBN), but the 12% yield from this route was impractical.

As Scheme 2 illustrates, treatment of (dadi)Ti(THF) (**1**-THF) with 1 equiv of SnX_4 provided the dihalides (dadi)TiX$_2$ (**2**-X$_2$, X = Cl, Br, I) as green and brown materials in modest yields (46−56%). In these cases, dihalides **2**-X$_2$ could be easily separated and crystallized from unidentified tin-containing byproducts. Each dihalide showed NMR spectral characteristics consistent with C_{2v} symmetry.

*dadi^{2-} as an Electrophile: (bida)TiCl$_2$ (**4**-Cl$_2$).* Standard thermolysis of **2**-Cl$_2$ as a stability test revealed the growth of a clean product that possessed only one mirror plane by ^{1}H NMR spectroscopy and included the appearance of a singlet (δ 4.88) integrating as 2 H. $^{13}C\{^1H\}$ NMR spectra also revealed a downfield resonance (δ 160.09) consistent with an aromatic (benzimidazole) carbon devoid of hydrogens. A single crystal X-ray diffraction experiment revealed a rearrangement in which an amide arm of the dadi^{2-} ligand attacked the imine backbone to afford a benzimidazole diamide tridentate chelate (bida). The yellow complex, $[\kappa^3\text{-}N,N,N,(2,6\text{-}^iPr_2C_6H_3)\text{-}C_6H_4NCH_2\{C(2,5\text{-}N,N(2,6\text{-}^iPr_2C_6H_3)C_6H_4\}]TiCl_2$((bida)-TiCl$_2$, **4**-Cl$_2$), was isolated in 80% yield, but sealed-tube experiments show that it forms nearly quantitatively, according to NMR spectral analysis.

Scheme 2. Synthesis of (dadi)TiX$_2$ (2-X$_2$, X = Cl, Br, I) and Dichloride Rearrangement Product (bida)TiCl$_2$ (4-Cl$_2$)

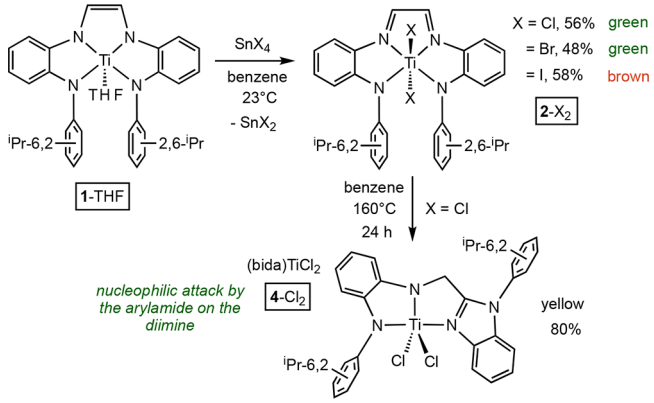

*Structure of (dadi)TiBr$_2$ (**2**-Br$_2$).* A limited set of metric data for (dadi)TiBr$_2$ (**2**-Br$_2$) is given in the caption of Figure 5,

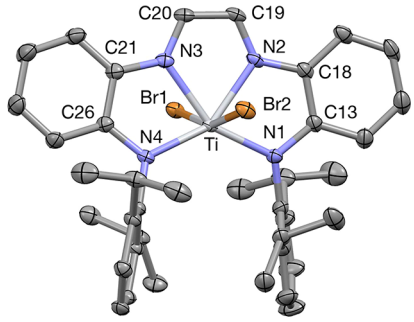

Figure 5. Molecular view of (dadi)TiBr$_2$ (**2**-Br$_2$). Selected distances (Å) and angles (deg): Ti−N1, 2.0063(19); Ti−N2, 2.1331(18); Ti−N3, 2.1352(19); Ti−N4, 2.0052(18); Ti−Br1, 2.5407(4); Ti−Br2, 2.5255(4); N2−C19, 1.316(3); N3−C20, 1.312(3); C19−C20, 1.416(3); N1−Ti−N2, 78.12(8); N1−Ti−N3, 150.31(8); N1−Ti−N4, 131.51(8); N2−Ti−N3, 72.48(7); N2−Ti−N4, 150.38(8); N3−Ti−N4, 77.98(7); Br1−Ti−N1, 93.17(5); Br1−Ti−N2, 84.71(5); Br1−Ti−N3, 80.27(5); Br1−Ti−N4, 92.60(5); Br2−Ti−N1, 94.15(6); Br2−Ti−N2, 80.33(5); Br2−Ti−N3, 85.05(5); Br2−Ti−N4, 95.12(5); Br1−Ti−Br2, 161.616(18).

which provides a molecular view of the pseudo-octahedral complex and its *trans*-dibromide configuration. The bromines are bent slightly away from the aryl isopropyl groups such that the H···Br interactions are at or longer than the sum of van der Waals radii (3.05−6.62 Å). The Br−Ti−Br angle is 161.62(2)°, and the N1/N4−Ti−Br1/Br2 angles average 93.8(11)° in corroboration of the steric effects. The remainder of the core is standard for a (dadi)$^{2-}$ ligand,[16] with *d*(C═N) of 1.316(3) and 1.312(3) Å, and a *d*(C19−C20) of 1.416(3) Å corresponding to an sp^2−sp^2 carbon−carbon single bond.[21] In addition, the *d*(Ti−N) for the amides average 2.0058(8) Å, which is considerably shorter than the corresponding distances to the imine nitrogens (2.1342(15) Å (avg)).

*Structure of (bida)TiCl$_2$ (**4**-Cl$_2$).* A molecular view of (bida)TiCl$_2$ (**4**-Cl$_2$) is illustrated in Figure 6, and it shows the pseudosquare pyramidal geometry of the complex, which has an Addison parameter of 0.27.[22] Data collection and

DOI: 10.1021/acs.organomet.8b00930
Organometallics 2019, 38, 1502−1515

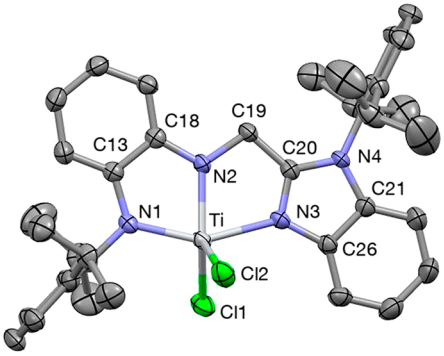

Figure 6. Molecular view of (bida)$TiCl_2$ (**4**-Cl_2). Selected distances (Å) and angles (deg): Ti−N1, 1.955(2); Ti−N2, 1.978(2); Ti−N3, 2.138(2); Ti−Cl1, 2.2579(11); Ti−Cl2, 2.2519(10); N1−C13, 1.398(3); C13−C18, 1.411(4); N2−C18, 1.388(4); N2−C19, 1.458(3); C19−C20, 1.463(4); N3−C20, 1.322(3); N4−C20, 1.352(3); N1−Ti−N2, 77.49(9); N1−Ti−N3, 151.72(9); N1−Ti−Cl1, 102.44(8); N1−Ti−Cl2, 105.66(7); N2−Ti−N3, 75.07(9); N2−Ti−Cl1, 135.58(8); N2−Ti−Cl2, 115.11(8); N3−Ti−Cl1, 92.45(7); N3−Ti−Cl2, 92.19(7); Cl1−Ti−Cl2, 107.69(4).

refinement information are given as Supporting Information, and a partial list of bond distances and interatomic angles is given in the caption to Figure 6. Bite angles of the diamide (77.49(9)°) and amide-imidazole (75.07(9)°) linkages cause the *N,N,N*-atoms of the tridentate chelate to bend. As a consequence, the N1−Ti−N3 angle is far from linear at 151.72(9)°, yet approximately the sum of the respective bite angles. One chlorine is slightly out of the N_3Ti plane (∠N2−Ti−Cl1 = 135.58(8)°), but the remaining core angles of ∠N2−Ti−Cl2 = 115.11(8)°, ∠Cl1−Ti−Cl2 = 107.69(4)°, ∠N1−Ti−Cl2 = 105.66(7)°, and ∠N3−Ti−Cl2 = 92.19(7)° clearly support the distorted square planar geometry. Titanium−nitrogen distances corresponding to the diamides are 1.955(2) and 1.978(2) Å, reflecting their anionic character, which contrasts with the neutral donor benzimidazole *d*(Ti−N3) of 2.138(2) Å.

Additions of RX (X = halide) to (dadi)Ti(THF) (1-THF). *(R-ita)TiX (**5**-RX; R = Me, Bn; X = Cl, Br).* Treatment of (dadi)Ti(THF) (**1**) with RX (R = Me, Bn; X = Cl, Br) for 24−36 h at 23 °C afforded brown imine-triamide complexes (R-ita)TiX (**5**-RX; R = Me, Bn; X = Cl, Br; R-ita = [{−CH_2*N*(1,2-C_6H_4)N(2,6-^{i}Pr$_2$-C_6H_3)}{CR = N(1,2-C_6H_4)N(2,6-^{i}Pr$_2$-C_6H_3)}]) as illustrated in Scheme 3. ^{1}H NMR spectra of the complexes reveal four different isopropyl groups indicative of no mirror planes, and a telltale doublet of doublets corresponding to the unique CH_2 unit of the imine-triamide, whose geminal coupling constants are large as a consequence of neighboring imine group:[25] **5**-MeCl, δ 5.18, 5.41, J_{gem} = 23.7 Hz; **5**-MeBr, δ 5.24, 5.42, J_{gem} = 24.3 Hz; **5**-BnCl, δ 5.07, 5.30, J_{gem} = 24.6 Hz; **5**-BnBr, δ 5.08, 5.29, J_{gem} = 24.6 Hz.

*Structure of (Me-ita)TiCl (**5**-MeCl).* A molecular view of (Me-ita)TiCl (**5**-MeCl) is illustrated in Figure 7, and its

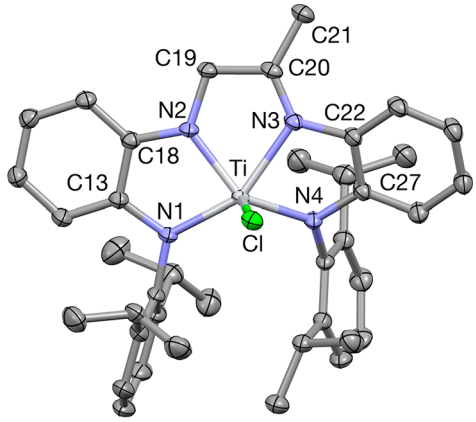

Figure 7. Molecular view of (Me-ida)TiCl (**5**-Cl). Selected distances (Å) and angles (deg): Ti−N1, 1.9798(12); Ti−N2, 1.9748(12); Ti−N3, 2.1539(12); Ti−N4, 1.9729(12); Ti−Cl, 2.2804(4); N1−C13, 1.4021(19); C13−C18, 1.4220(19); N2−C18, 1.3886(18); N2−C19, 1.4507(17); C19−C20, 1.487(2); C20−C21, 1.4956(19); N3−C20, 1.2881(19); N3−C22, 1.4202(19); C22−C27, 1.411(2); N4−C27, 1.4116(18); N1−Ti−N2, 78.99(5); N1−Ti−N3, 150.40(5); N1−Ti−N4, 118.68(5); N2−Ti−N3, 73.14(5); N2−Ti−N4, 134.40(5); N3−Ti−N4, 76.50(5); N1−Ti−Cl, 106.34(4); N2−Ti−Cl, 108.73(4); N3−Ti−Cl, 92.07(3); N4−Ti−Cl, 105.54(4).

pseudo-square pyramidal geometry (τ = 0.27)[22] is clearly represented. As the caption indicates, the three titanium-amide *d*(Ti−N) distances of 1.9798(12), 1.9748(12) and 1.9729(12) Å are distinct from the titanium-imine nitrogen bond length of 2.1539(12) Å. The *d*(CN) of the imine is 1.2881(19) Å, which easily differentiates it from the N−C(sp^3) distance of 1.4507 Å.[21] The chloride is tilted slightly toward the imine, as ∠N3−Ti−Cl = 92.07(3)° contrasts with the chloride angles relative to the amide nitrogens, which average 106.9(17)°. The core angles reveal the standard diamide "bite" of ∠N1−Ti−N2 = 78.99(5)°, while the backbone "bite" of 73.14(5)° is essentially unchanged from the dadi ligand, despite the conversion to an amide-imine. The open end of Me-ita has ∠N1−Ti−N4 = 118.68(5)°, which is similar to that of dimer **3**, but less open by ∼14° than the dadi^{2-} ligand in **2**-Br_2.

*Structure of (Bn-ita)TiCl (**5**-BnCl).* A different perspective of the oxidative addition product (Bn-ida)TiCl (**5**-BnCl) is illustrated in Figure 8, but the metrics, which can be found in

Scheme 3. Additions of RX to (dadi)Ti(THF) (1) Afford Products Containing New C−C Bonds

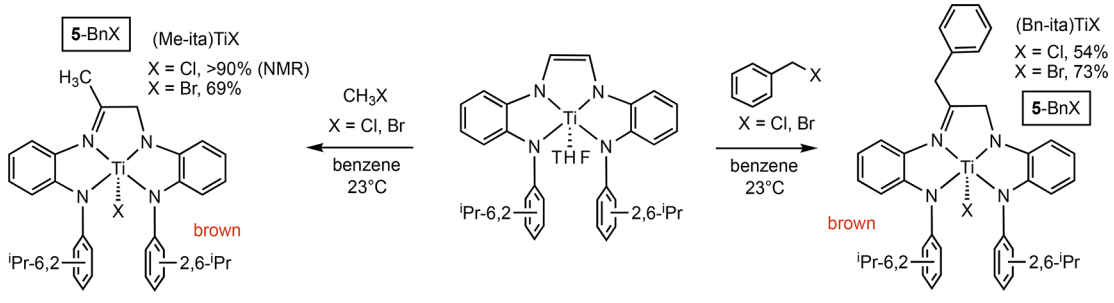

DOI: 10.1021/acs.organomet.8b00930
Organometallics 2019, 38, 1502−1515

the caption, are basically the same. The complex is a distorted square pyramid with an Addison parameter of $\tau = 0.27$.[21]

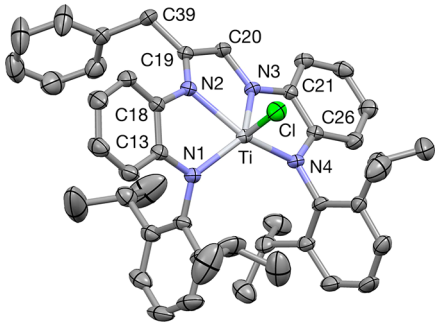

Figure 8. Molecular view of (Bn-ida)TiCl (**5**-BnCl). Selected distances (Å) and angles (deg): Ti−N1, 1.9848(18); Ti−N2, 2.1584(18); Ti−N3, 1.9785(18); Ti−N4, 1.9790(18); Ti−Cl, 2.2750(7); N1−C13, 1.417(3); C13−C18, 1.409(3); N2−C18, 1.423(3); N2−C19, 1.291(3); C19−C20, 1.479(3); C19−C39, 1.507(3); N3−C20, 1.445(3); N3−C21, 1.395(3); C21−C26, 1.413(3); N4−C27, 1.452(3); N1−Ti−N2, 76.66(7); N1−Ti−N3, 134.23(8); N1−Ti−N4, 121.02(7); N2−Ti−N3, 72.99(7); N2−Ti−N4, 150.51(7); N3−Ti−N4, 78.37(5); N1−Ti−Cl, 105.18(4); N2−Ti−Cl, 91.48(5); N3−Ti−Cl, 109.02(6); N4−Ti−Cl, 104.51(5).

Mechanisms of RX Addition to (dadi)Ti(THF) (1-THF). *Radical Chain.* The disposition of the alkyl and halide components in (R-ita)TiX (**5**-RX; R = Me, Bn; X = Cl, Br) prompted consideration of a radical chain process in which halide abstraction can serve as an initiation step. As Scheme 4 indicates, a subsequent alkyl radical attack on the dadi backbone affords a triamide imine Ti(III) species that can also abstract halogen, regenerating the propagating R•. The usual termination steps are invoked, including recombination of the initiation products to generate **5**-RX. At some point during the process, a 1,2-H shift is necessary to provide the correct regiochemistry. Mashima et al. have observed a related rearrangement subsequent to radical RX addition in a tantalum diimine system.[26]

Several factors implicated a radical process.[27−35] Attempts to measure rates of oxidative addition were hampered by the sporadic nature of the reaction. It was generally the case that the benzyl halides reacted faster than the methyl halides and that the bromide substrates were faster than the chlorides,[27] but statistically significant rate data could not be obtained. Multiple additions of BnBr to (dadi)Ti(THF) (**1**-THF) had varied rates, but were typically complete within <15 min at 23 °C (1−10 equiv of BnBr; $\Delta G^{\ddagger}$(max) ∼ 20−21 kcal/mol), hampering monitoring, and efforts to determine phenomenological rate data were abandoned. Radical inhibitors (9,10-dihydroanthracene, 1,4-cyclohexadiene) attenuated reactivity, but given the random rates of reaction, these supported, but were not significant evidence of, radical reactivity.

Suspicion regarding radical paths was immediately raised when (dadi)Ti(THF) (**1**-THF) failed to react with ^{t}BuBr, a substrate that would normally generate a Ti−Br bond, and *tert*-butyl radical products such as isobutylene, isobutane, and 2,2,3,3-tetramethylbutane.[29] Contrast this result with the NMR tube scale addition of ^{i}PrBr to **1**-THF,[30] which generated the standard product, (^{i}Pr-ita)TiBr (**5**-^{i}PrBr), in ∼80% purity as illustrated in Scheme 5. With the mechanism now in question, radical clocks were tested as substrates that can be indicative of radical reactions via well-known rearrangements. Two typical clock precursors were chosen: 5-hexenyl bromide (k(cyclization, 25 °C) of 5-hexenyl-radical ∼2.3×10^{5} s^{-1}), and cyclopropylmethyl bromide (k(ring-opening, 25 °C) of cyclopropylmethyl-radical ∼1.3×10^{8} s^{-1}).[36,37] As Scheme 5 indicates, NMR tube experiments conducted with these probes found no evidence of a cyclized product in the former, nor a ring-opened product in the latter. Treatment of **1**-THF with 5-hexenyl bromide produced (5-hexenyl-ita)TiBr (**5**-HxBr; δ 4.53, 4.80, J_{gem} = 24.0 Hz), while addition of ^{c}PrCH$_2$Br generated (^{c}PrCH$_2$−ita)TiBr (**5**-^{c}PrCH$_2$Br; δ 4.84, 4.98, J_{gem} = 24.2 Hz) and both products manifested the diagnostic large geminal coupling by the ligand backbone methylene group. In the lowest possible concentration analytically feasible, ([**1**-THF] = 0.002 M), it is estimated that the rate of a radical process (e.g., ^{c}PrCH$_2$· + **1**-THF; k_{trap}[^{c}Pr][**1**-THF]) would have to be $k_{trap} \geq 1.1 \times 10^{10}$ M^{-1} s^{-1}. Since this is essentially diffusion-controlled, it was deemed very unlikely, and focus was now directed toward alkylation paths of a concerted nature.

*Structure of (^{c}PrCH$_2$−ita)TiBr (**5**-^{c}PrCH$_2$Br).* Crystals harvested from the NMR tube reaction involving ^{c}PrCH$_2$Br were subjected to single crystal X-ray structural analysis, and further proof of the cyclopropylmethyl derivative, (^{c}PrCH$_2$−

Scheme 4. Radical Chain Path Considered for the Formation of (R-ita)TiX (5-RX; R = Me, Bn; X = Cl, Br)

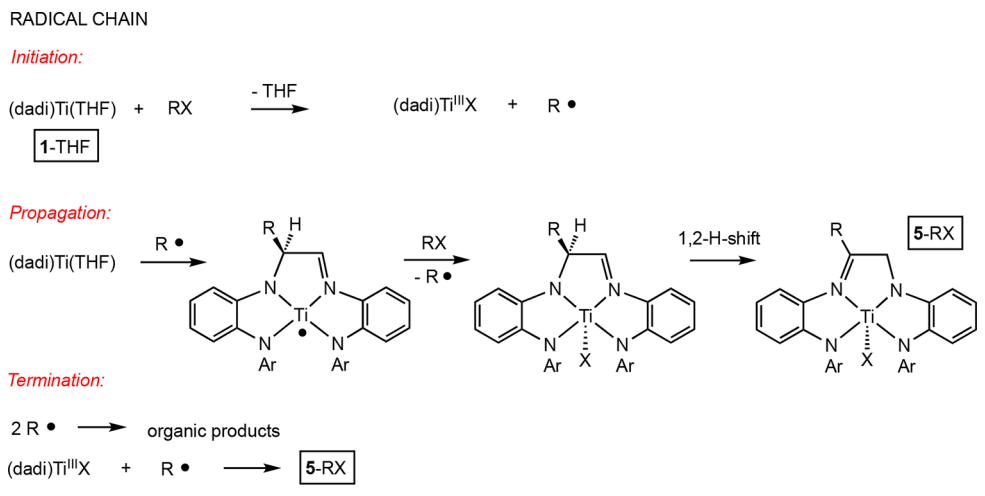

DOI: 10.1021/acs.organomet.8b00930
Organometallics 2019, 38, 1502−1515

Scheme 5. Secondary, Tertiary, And Radical Clock Alkylbromides and (dadi)Ti(THF) (1-THF)

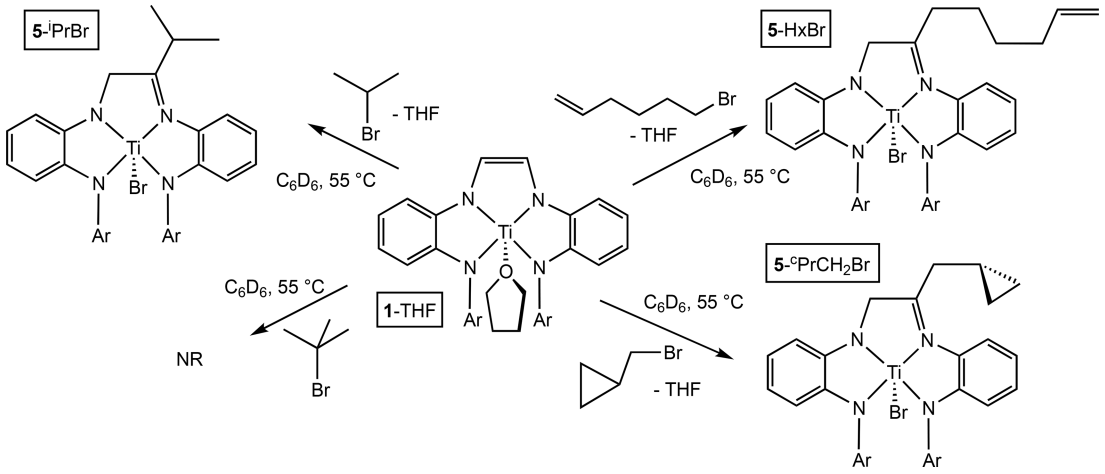

ita)TiBr (**5**-^{c}PrCH$_2$Br), was obtained. Figure 9 illustrates the now-familiar triamide-imine structure, which is a distorted square pyramid with a capping bromide, similar to that in Figures 7 and 8. The metric features of **5**-^{c}PrCH$_2$Br were similar to the related previous structures, and its Addison parameter is τ = 0.28.[22]

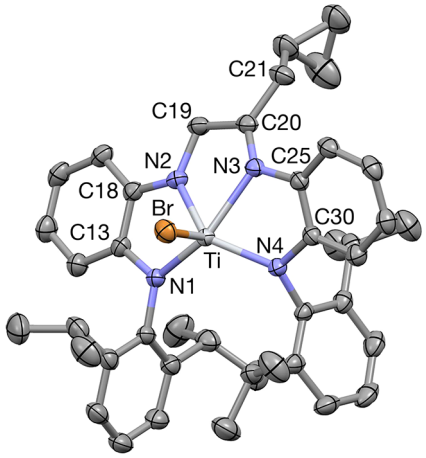

Figure 9. Molecular view of (^{c}PrCH$_2$–ida)TiCl (**5**-^{c}PrCH$_2$Br). Selected distances (Å) and angles (deg): Ti–N1, 1.9816(12); Ti–N2, 1.9664(12); Ti–N3, 2.1671(11); Ti–N4, 1.9695(11); Ti–Br, 2.4406(3); N1–C13, 1.4096(18); C13–C18, 1.416(2); N2–C18, 1.3887(19); N2–C19, 1.4481(18); C19–C20, 1.490(2); C19–C39, 1.508(2); N3–C20, 1.2887(19); N3–C25, 1.4219(17); C25–C30, 1.4049(19); N4–C30, 1.4159(17); N1–Ti–N2, 79.48(5); N1–Ti–N3, 150.54(5); N1–Ti–N4, 117.27(5); N2–Ti–N3, 73.17(5); N2–Ti–N4, 133.52(5); N3–Ti–N4, 76.33(5); N1–Ti–Br, 107.23(4); N2–Ti–Br, 108.94(4); N3–Ti–Br, 92.06(3); N4–Ti–Br, 106.36(4).

Oxidative Addition and Concerted 3 + 2 Mechanisms. Given the results in Scheme 5, concerted pathways[27−35] for the addition of RX to (dadi)Ti(THF) (**1**-THF) were considered. Since experiments with these highly sensitive and reactive titanium species have intrinsic limitations, and no intermediates were detected, calculations were utilized to assess certain mechanisms with BnBr as the prototypical substrate. Since its phenomenological reaction rate was found to have maximum barrier of ∼20−21 kcal/mol, this serves as a benchmark for the calculations.

Scheme 6 illustrates a standard oxidative addition to titanium followed by a migratory insertion into the imine, and subsequent 1,2-H shift as one concerted path. The transition state for oxidative addition of BnBr to **1**-THF, which can be viewed as dissociative loss of THF (ΔG°_{calc} = +20.9 kcal/mol relative to **1**-THF at 0.0 kcal/mol), followed by BnBr adduct formation (e.g., (dadi)Ti(BrBn) (**1**-BrBn) at ∼6 kcal/mol) and addition to afford a *cis*- or *trans*-(dadi)Ti(Bn)Br species at 13.1 or −1.4 kcal/mol, respectively, was calculated to be $\Delta G^{\ddagger}$ = 27.7 kcal/mol. While the first C-alkylation intermediate is exergonic from the *trans* oxidative addition intermediate, *trans*-(dadi)Ti(Bn)Br, by −23.9 kcal/mol, the barrier to migration appears prohibitive (>28 kcal/mol (calc)). The concerted 3 + 2 BnBr addition, the second mechanism shown in Scheme 6, is also tentatively ruled out on a similar basis.

Polar Mechanisms: Dadi^{4-} as a Nucleophile. The polar addition processes looked promising, and two similar processes are considered. In the polar oxidative addition mechanism via direct alkylation of [(dadi)TiCl]$^{-}$, some generation of chloride permits substitution of THF from **1**-THF to afford the anion [(dadi)TiCl]$^{-}$, and this is the propagating agent of a chain process that involves alkylation of dadi^{4-}(a formal ligand oxidation) and regeneration of the halide anion. This process can be independently tested, and treatment of [(dadi)TiCl]Li (**1**-ClLi)[16] with BnCl at 23 °C afforded an alkylation product within 15 min. 2D NMR spectroscopy revealed it to be a single alkylation product (H-Bn-ita)TiCl (**5′**-BnCl), but with the connectivity of the presumed first-formed species, as Scheme 7 indicates. Heating at 55 °C induced the shift[26] to the final product, (Bn-ita)TiCl (**5**-BnCl), in essentially quantitative yield. It is crucial to note that the barrier for the isomeric conversion was measured to be ∼24 kcal/mol at 55 °C; hence, this 1,2-H shift is ruled out as a path in the BnX oxidative additions, since **5′**-BnX should be observed in these experiments but is not. Furthermore, calculations on the 1,2-H shift converting **5′**-BnBr to **5**-BnBr show the barriers to be higher than 24 kcal/mol, and essentially the same whether the Bn and Br groups are syn ($\Delta G^{\ddagger}$ = 28.4 kcal/mol) or anti ($\Delta G^{\ddagger}$ = 29.7 kcal/mol) with respect to the N$_4$Ti plane. Isomerization paths based on β-H-elimination from amide **5′**-BnBr are also calculated to have barriers significantly higher than 24 kcal/mol.

DOI: 10.1021/acs.organomet.8b00930
Organometallics 2019, 38, 1502−1515

Scheme 6. Concerted and Polar Paths for the Formation of (R-ita)TiX (5-RX; R = Me, Bn; X = Cl, Br)

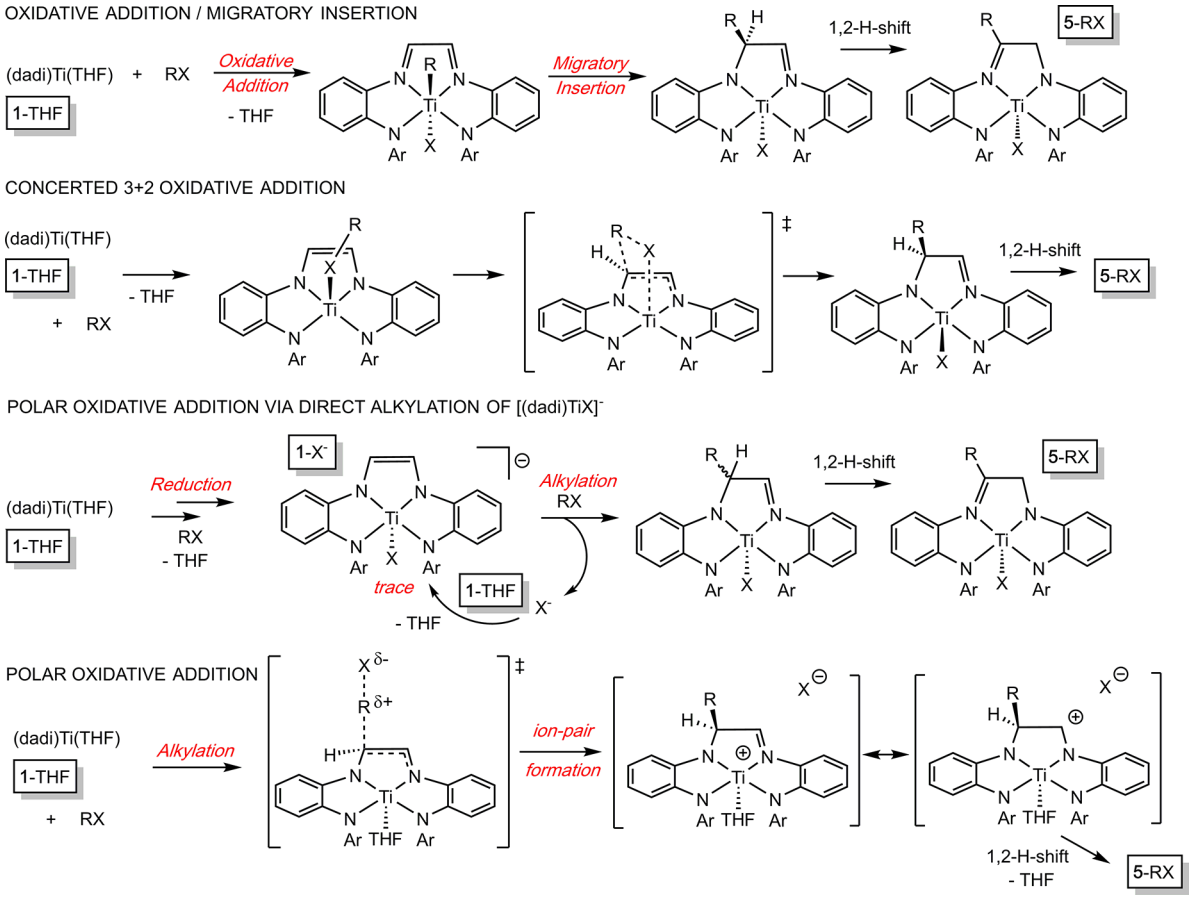

Scheme 7. Concerted and Polar Paths for the Formation of (R-ita)TiX (5-RX; R = Me, Bn; X = Cl, Br)

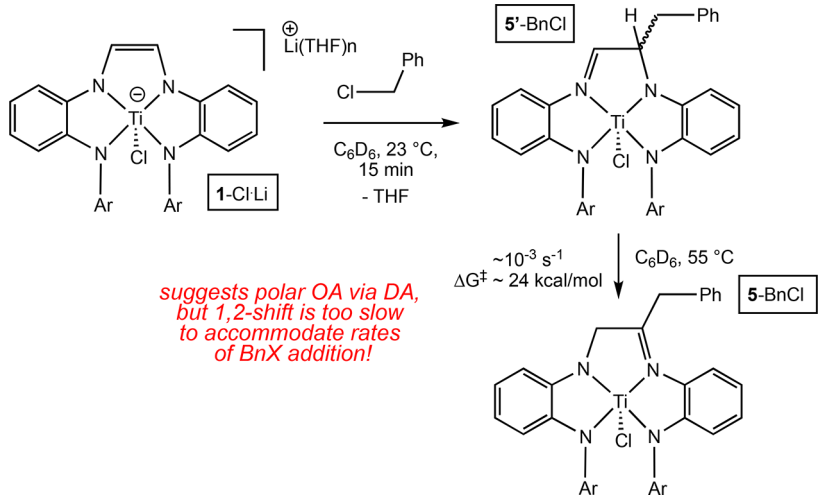

Of the proposed mechanisms, only the polar oxidative addition to **1**-THF remains. While similar to the previous mechanism with regard to the alkylation, it is not a chain process. Initial C−C bond formation is propsed to generate an ion-pair analogous to related RX additions of square planar d^8 complexes.[27−34] Calculations on the 1,2-H shift suggest it again has too high a barrier (~30 kcal/mol), but in this instance, activity of the counteranion may play a role, a factor that was difficult to test with high veracity. It is also feasible that alkylation and 1,2-H shift occur concomitantly. The ion-pair must be invoked because free halide would likely convert **1**-THF to **1**-X^-,[16] which should induce the reactivity shown in Scheme 7 that was ruled out by no observation of **5′**-RX.

Mechanism of Dimer *trans*-C_6H_4-{1,2-(*N*,2-*N*(2,6-^{i}Pr$_2$-C_6H_3)-C_6H_4)$_2$Ti-NHAd}$_2$ (3) Formation. *Source of the* $-CH_2-$ *Units.* A breakthrough in the mystery surrounding the formation of *trans*-C_6H_4-{1,2-(*N*,2-*N*(2,6-^{i}Pr$_2$-C_6H_3)-C_6H_4)$_2$Ti-NHAd}$_2$ (**3**) occurred when a ~2 year old NMR tube-scale reaction of (dadi)Ti═NAd (**2**═NAd) with 0.5 equiv of $P(CD_3)_3$ was discovered to have deposited a

DOI: 10.1021/acs.organomet.8b00930
Organometallics 2019, 38, 1502−1515

microcrystalline solid, identified as **3**-d_6. ^{1}H NMR spectral analysis indicated substantial deuterium incorporation at the methylene positions of the C_6-bridging ring (50−70% and >90%), collapse of the multiplet corresponding to the adjacent methine, and 75−80% deuterium in the amide positions, as Scheme 8 indicates. The $P(CD_3)_3$ reaction was conducted

Scheme 8. Reaction of (dadi)Ti═NAd (2═NAd) with 0.5 equiv of $P(CD_3)_3$ Revealed the Phosphine As the Source of the C_6-Ring Methylenes

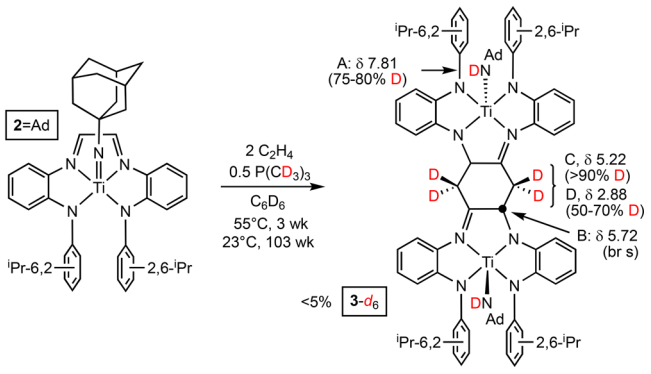

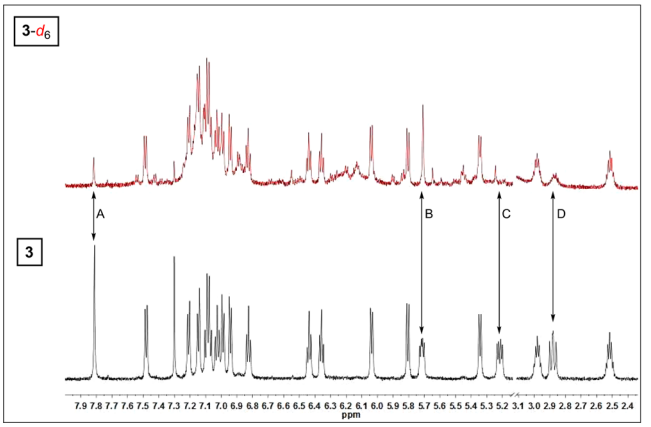

mostly at a lower temperature (3 weeks at 55 °C, 103 weeks at 23 °C), and may have steps involving CH/D abstraction, consistent with large kinetic isotope effects leading to its lengthy deposition time.

Dimerization. Observation of the triamide-imine regiochemistry pertaining to the (R-ita)TiX (**5**-RX; X = Br, R = Me, Bn, ^{i}Pr, $CH_2{}^c$Pr, 5-hexenyl; X = Cl, R = Me, Bn) complexes suggested a means of dimerization leading to the formation of *trans*-C_6H_4-{1,2-(*N*,2-*N*(2,6-^{i}Pr$_2$-C_6H_3)-C_6H_4)$_2$Ti-NHAd}$_2$ (**3**). As Figure 10 illustrates, the generation of an oxidative addition product ((YCH$_2$)-ita)TiNHAd should be subject to HY-elimination leading to the formation of an eneamide-imine intermediate. Subsequent dimerization via attack of the nucleophilic eneamide on the electrophilic imine of another titanium intermediate would lead directly to **3**. Related nucleophile/electrophile couplings of 1,3-di-(2-pyridyl)-2-azaallyl (smif) constituents and others[6−12] have been postulated as nonradical alternatives in the C−C bond forming steps illustrated in Figure 1.

Intermediate Model. If the eneamide-imine coupling mechanism is operational, then an intermediate capable of undergoing HY elimination according to Figure 9 is necessary. Scheme 9 illustrates a plausible precursor to an eneamine-imine precursor, as the treatment of (dadi)Ti(THF) (**1**-THF) with Ph_2PCH_2Cl led to the isolation of (Ph_2PCH_2−ita)TiCl (**5**-(CH_2P')Cl) in 59% yield. In the generation of **3**, the Y component would be −CH_2PMePh, but synthesis of the diphenyl(chloromethyl)phosphine was less problematic and leads to only one diastereomer. A dimer related to **3**, but with chloride in place of the adamantyl amide, was the target of thermolysis of **5**-(CH_2P')Cl, but a complex mixture of products was produced. Since the solubility of a chloride dimer analogous to **3** is expected to be quite low, it may not be soluble enough to be detected. Identification of a trace amount of (Me-ita)TiCl (**5**-MeCl) indicated that phosphine elimination was plausible.

dadi^{2-} as an Electrophile. During the course of investigating potential impurities as initiators or inhibitors affecting the formation of *trans*-C_6H_4-{1,2-(*N*,2-*N*(2,6-^{i}Pr$_2$-C_6H_3)-C_6H_4)$_2$Ti-NHAd}$_2$ (**3**), (dadi)Ti═NAd (**2**═NAd) was initially exposed to $PhMe_2PO$ in the presence of $PhMe_2P$. NMR spectral analysis of the reaction indicated the formation of a previously unobserved product. As a consequence, **2**═NAd was treated with $PhMe_2PO$ at 23 °C for 18 h, and rearrangement to the benzimidazole diamide tridentate chelate was observed, concomitant with phosphine oxide binding, to afford green (bida)Ti═NAd(OPMe$_2$Ph) (**6**, 69%):

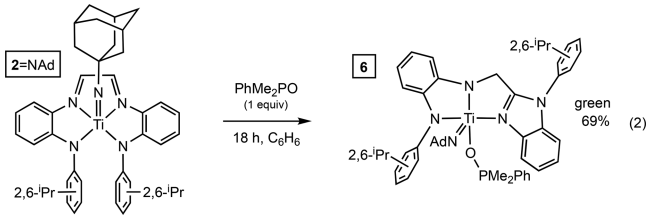

In both cases of dadi^{2-} rearrangement to the (bida)$^{2-}$ ligand, a backbone imine serves as an electrophile and is nucleophilically attacked by an amide arm of the chelate.

*Structure of (bida)Ti═NAd(OPMe$_2$Ph) (**6**).* Figure 11 illustrates a molecular view of (bida)Ti═NAd(OPMe$_2$Ph) (**6**), revealing its pseudo-square pyramidal (τ = 0.16)[22] geometry. The metrics of the bida ligand can be found in

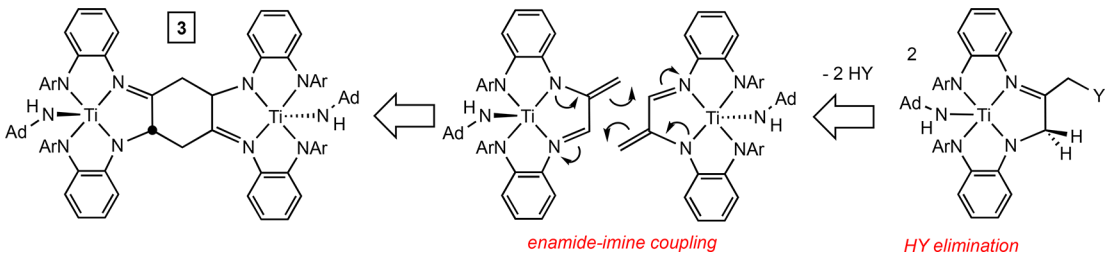

Figure 10. Plausible enamide-imine coupling dimerization step for formation of **3**.

DOI: 10.1021/acs.organomet.8b00930
Organometallics 2019, 38, 1502−1515

Scheme 9. Ph_2PCH_2Cl Oxidative Addition to (dadi)Ti(THF) (1-THF) Yields an Elimination Model

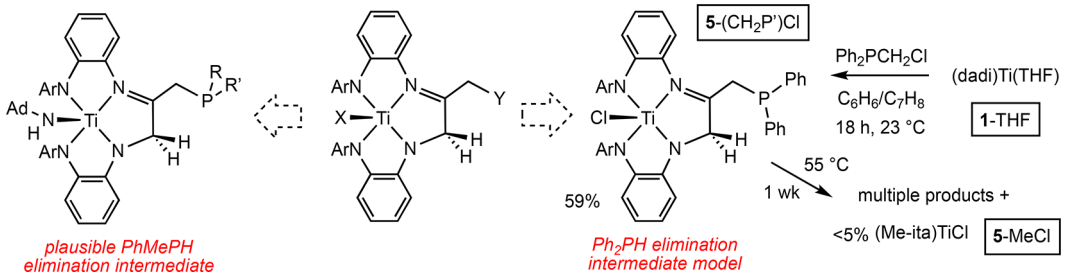

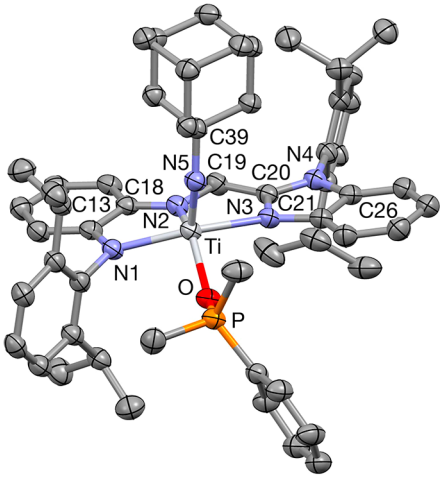

Figure 11. Molecular view of (bida)Ti=NAd($OPMe_2Ph$) (**6**). Selected distances (Å) and angles (deg): Ti–N1, 2.090(2); Ti–N2, 2.042(2); Ti–N3, 2.222(2); Ti–N5, 1.722(2); Ti–O, 2.0351(19); N1–C13, 1.388(3); C13–C18, 1.429(4); N2–C18, 1.373(3); N2–C19, 1.439(3); C19–C20, 1.483(4); N3–C20, 1.328(3); N4–C20, 1.362(3); P–O, 1.5143(19); N5–C39, 1.443(3); N1–Ti–N2, 76.38(9); N1–Ti–N3, 146.91(9); N1–Ti–N5, 109.80(10); N1–Ti–O, 95.10(8); N2–Ti–N3, 74.26(8); N2–Ti–N5, 114.09(10); N2–Ti–O, 137.60(8); N3–Ti–N5, 95.98(10); N3–Ti–O, 96.32(8); N5–Ti–O, 107.91(9); Ti–N5–C39, 157.73(19); Ti–O–P, 138.36(12).

the caption, and they are quite similar to those pertaining to (bida)$TiCl_2$ (**4**-Cl_2). The d(Ti–N) of 2.090(2) (N1), 2.042(2) (N2), and 2.222 (2) Å (N3) are 0.135, 0.064, and 0.084 Å longer than in **4**-Cl_2, influenced by the stronger imide and phosphine oxide donation relative to chloride. The titanium imide bond length of 1.722(2) Å is normal,[16,38,39] and the d(Ti–O) of 2.0351(19) Å is indicative of a strong interaction. The core angles, listed in the Figure 11 caption, are quite similar to **4**-Cl_2 and are not unusual.

*Plausible Mechanism for Generation of **3**.* The exploration of oxidative addition chemistry pertaining to (dadi)Ti(THF) (**1**-THF) was predicated on the likelihood that radicals were involved in the mechanism of dimer *trans*-C_6H_4-{1,2-(*N*,2-*N*(2,6-^{i}Pr_2-C_6H_3)-C_6H_4)$_2$Ti-NHAd}$_2$ (**3**) formation. Neither the oxidative addition studies nor reactivity studies of (dadi)Ti=NAd (**2**=NAd) have conclusively shown that radical chemistry is evident. Fortunately, valuable insight into the mechanism of the formation of **3** comes from the labeling study involving **2**=NAd and $P(CD_3)_3$, illustrated in Scheme 8. The prolonged reaction times and low yields have hampered investigations, such that the initial steps in the process remain unknown, and radical chemistry cannot be ruled out.

The sporadic nature of dimerization, especially the PMe_2Ph batch dependence on product formation, keeps radical reactivity forefront in the discussion (Scheme 10). Since phosphine is necessary for the reaction, it may help initiate the reaction by binding to the titanium and inducing imidyl character at the AdN ligand, which could initiate a radical process by abstracting a hydrogen atom (HAT) from another

Scheme 10. Potential Radical and Nucleophilic Steps to Initiate Dimer *trans*-C_6H_4-{1,2-(*N*,2-*N*(2,6-^{i}Pr_2-C_6H_3)-C_6H_4)$_2$Ti-NHAd}$_2$ (3) Formation

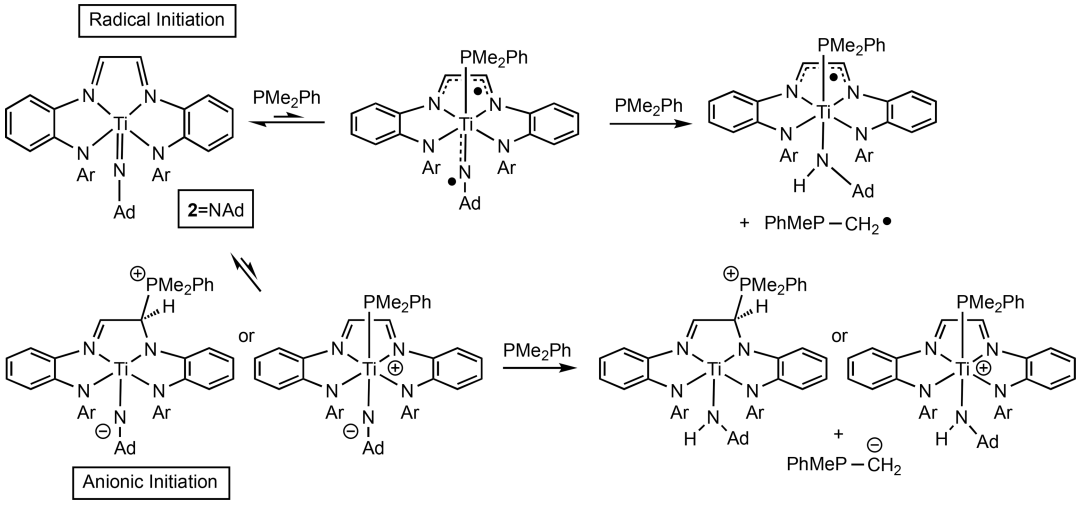

DOI: 10.1021/acs.organomet.8b00930
Organometallics 2019, 38, 1502–1515

Scheme 11. Potential Radical and Nucleophilic Propagation Steps toward Dimer *trans*-C_6H_4-{1,2-(*N*,2-*N*(2,6-^{i}Pr$_2$-C_6H_3)-C_6H_4)$_2$Ti-NHAd}$_2$ (3) Formation

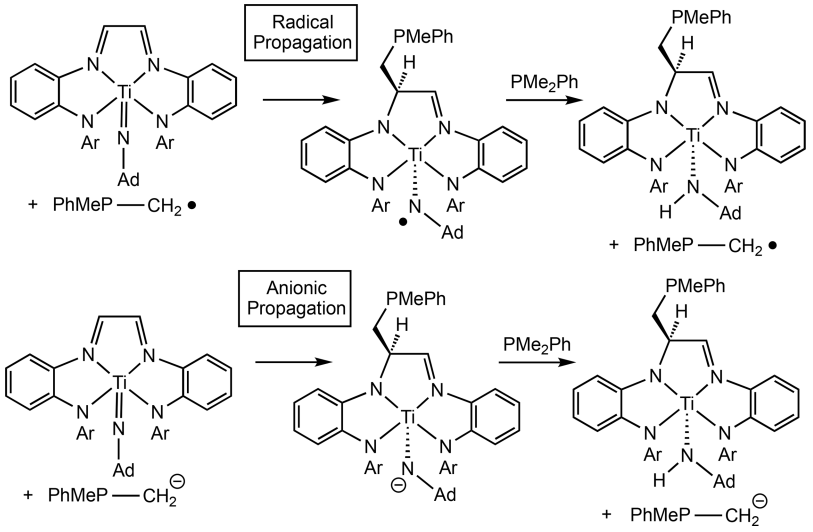

Scheme 12. Elimination of HPMePh to the Electrophile/Nucleophile and Subsequent Coupling To Give 3

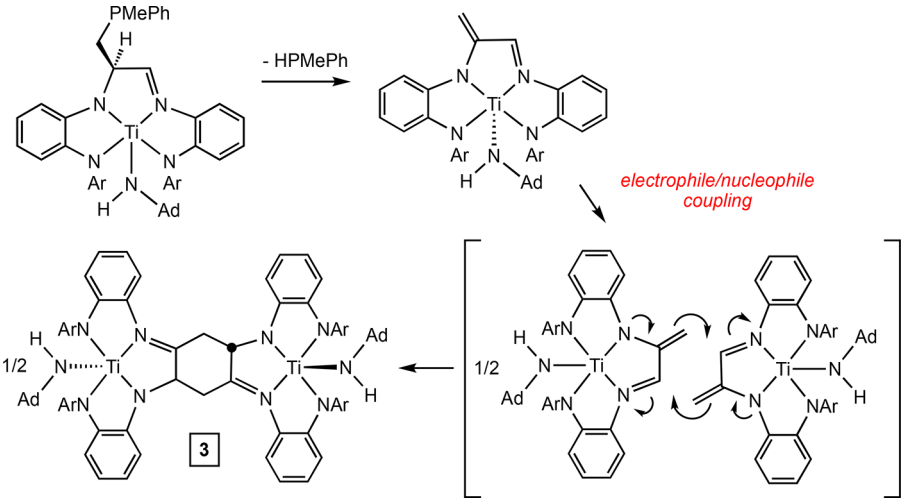

phosphine. Independent efforts to trigger and observe radical character (e.g., **1**-THF + PMe_2Ph + $HCPh_3$) proved uninformative. Alternatively, nucleophilic attack by the phosphine at either the metal or the dadi backbone can generate anionic character at the NAd, and deprotonation is a possibility. Even if HAT or deprotonation are endothermic events, the lengthy reaction time suggests that such steps are still feasible provided subsequent reactions are thermodynamically viable. In the proposed initiations, propagation agents, either the radical $PhMePCH_2\cdot$ or anion $PhMePCH_2^-$ are generated.

Scheme 11 illustrates probable radical (via $PhMePCH_2\cdot$) or anionic (via $PhMePCH_2^-$) propagation steps that show how the product amide is formed, and why deuterium incorporation was observed when $P(CD_3)_3$ was found to generate **3** (Scheme 8). Both propagations lead to addition of $-CH_2PMePh$ to the dadi backbone to form (H-($PhMePCH_2$)ita)TiNHAd, which is similar to addition product **5′**-BnCl that was generated from [(dadi)TiCl][Li(THF)$_4$] (**1**-ClLi) and BnCl. Since it has been determined that there is a significant barrier to the 1,2-H shift ($\Delta G^{\ddagger} \sim 24$ kcal/mol), a competing elimination of HPMePh affords the eneamide-imine as illustrated in Scheme 12. Dimerization of this species would lead to *trans*-C_6H_4-{1,2-(*N*,2-*N*(2,6-^{i}Pr$_2$-C_6H_3)-C_6H_4)$_2$Ti-NHAd}$_2$ (**3**) and rationalizes why its methylene groups possess deuterium when $P(CD_3)_3$ was present.

Ethylene is necessary for the overall process, but it is not incorporated in product. Any HPMePh formed upon elimination would likely interfere with either propagation step as its PH bond is relatively weak (BDE(cal'd) = 66.7 kcal/mol)[40] and more acidic (pK_a(cal'd) = 19)[41] than a phosphine methyl CH bond (BDE(cal'd) = 89.0 kcal/mol; pK_a = 40). It is plausible that C_2H_4 serves to scavenge HPMePh, perhaps catalyzed by the substantial detritus of the lengthy process, thereby preventing it from being a competing substrate. Analyses of the $^{31}P\{^1H\}$ NMR spectra under conditions where **3** is formed indicate the presence of myriad phosphorus-containing species.

CONCLUSIONS

The reactivity presented herein is consistent with the dadi^n ligand acting in a nucleophilic capacity as the tetraanion (dadi^{4-}) in (dadi)Ti(THF) (**1**-THF), and as an electrophile as the diimine dianion (dadi^{2-}) in (dadi)TiX_2 (**2**-X_2, X = Cl, Br,

DOI: 10.1021/acs.organomet.8b00930
Organometallics 2019, 38, 1502−1515

Scheme 13. Plausible Polar Oxidative Addition Mechanism of RX Addition to (dadi)Ti(THF) (1-THF) with Concomitant 1,2-H Shift

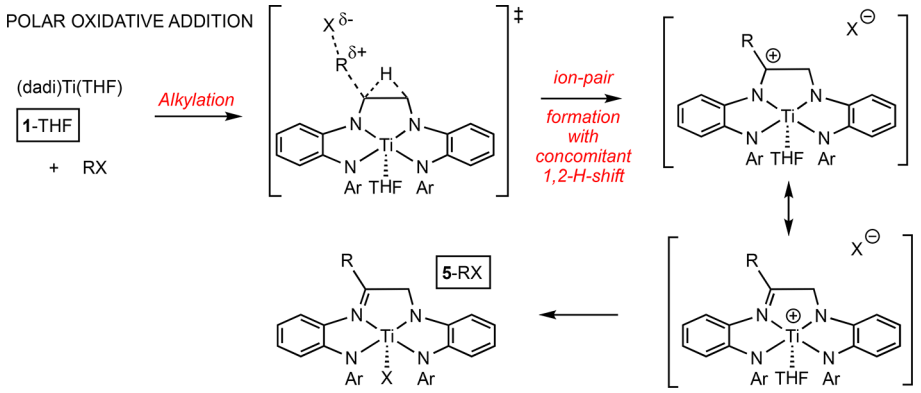

I) and (dadi)Ti═NAd (**2**═NAd). While clear indication of radical character in dadi^{3-}, as predicted by calculations of (dadi)Ti (**1**) (i.e., (dadi^{3-})$^{\uparrow}$Ti$^{III\downarrow}$) has not been realized, it is predicated on the generation of **1**, so loss of THF from **1**-THF could be a determining factor. The formation of dimer *trans*-C_6H_4-{1,2-(*N*,2-*N*(2,6-$^{i}Pr_2$-C_6H_3)-C_6H_4)$_2$Ti-NHAd}$_2$ (**3**) can involve the radical anion dadi^{3-} if phosphine binding induces imidyl character in **2**═NAd.

Despite significant effort, a general mechanism rationalizing oxidative addition of RX to (dadi)Ti (**1**) remains somewhat elusive. Sporadic reaction rates, while seeming indicative of a radical process, are likely to be an outcome of highly sensitive concerted process(es), since the lack of radical clock rearrangements rule out all but the swiftest ($k > 1.1 \times 10^{10}$ M^{-1} s^{-1}) of chain propagation events. One key observation was conversion of (H-Bn-ita)TiCl (**5′**-BnCl) to (Bn-ita)TiCl (**5**-BnCl), which possesses enough of a barrier to rule out any general mechanism requiring a fast 1,2-H shift (Schemes 4 and 6), including any radical process. Several nonradical paths were considered, but the former observation limits the possibilities to the polar oxidative addition mechanism, which undergoes a different 1,2-H shift. It occurs in a cation, or tight ion pair, and although calculations suggest that its barrier (≥24 kcal/mol) is similar to that measured and calculated for **5′**-BnCl to **5**-BnCl, the shift is difficult to accurately portray due to solvation effects that can influence the reaction rate. It is plausible that the 1,2-H shift occurs concurrent with alkylation, as Scheme 13 reveals. In this instance, the more substituted cation generated (RR′C(+)N) possesses greater stability than the unshifted, unsubstituted one (RHC(+)N).

Ambiguities also persist in the formation of dimer *trans*-C_6H_4-{1,2-(*N*,2-*N*(2,6-$^{i}Pr_2$-C_6H_3)-C_6H_4)$_2$Ti-NHAd}$_2$ (**3**), but the real problems are the intrinsic limitations of a low yield, long duration pathway. A reasonable mechanism, addressed in Schemes 10−12, concerns radical or basic activation of a methyl CH bond in Me_2PhP (or CD bond in $P(CD_3)_3$) in a chain process. The resulting (H-(PhMePCH$_2$)-ita)TiNHAd species can eliminate HPMePH to provide the key eneamide-imine that dimerizes to afford **3**.

EXPERIMENTAL SECTION

Full experimental details are given in the Supporting Information, including syntheses, mechanistic experiments (typically NMR-tube scale), spectroscopic data, X-ray crystal structure information, and general computational procedures. Qualitative descriptions of the synthetic experiments and crystallographic metric are given in the schemes and figures; all molecular views are drawn with 50% ellipsoids.

ASSOCIATED CONTENT

Supporting Information

The Supporting Information is available free of charge on the ACS Publications website at DOI: 10.1021/acs.organomet.8b00930.

Experimental, general considerations, procedures, NMR tube-scale reactions, mechanistic probes toward understanding dimer *trans*-C_6H_4-{1,2-(*N*,2-*N*(2,6-$^{i}Pr_2$-C_6H_3)-C_6H_4)$_2$Ti-NHAd}$_2$ (**3**) formation, X-ray crystal structures, calculations, and additional references (PDF)

Accession Codes

CCDC 1851274−1851279 and 1886264 contain the supplementary crystallographic data for this paper. These data can be obtained free of charge via www.ccdc.cam.ac.uk/data_request/cif, or by emailing data_request@ccdc.cam.ac.uk, or by contacting The Cambridge Crystallographic Data Centre, 12 Union Road, Cambridge CB2 1EZ, UK; fax: +44 1223 336033.

AUTHOR INFORMATION

Corresponding Author

*Tel.: 607-255-7220. E-mail: ptw2@cornell.edu (P.T.W.).

ORCID

Samantha N. MacMillan: 0000-0001-6516-1823
Thomas R. Cundari: 0000-0003-1822-6473
Peter T. Wolczanski: 0000-0003-4801-0614

Notes

The authors declare no competing financial interest.

ACKNOWLEDGMENTS

Support from the National Science Foundation (CHE-1402149; CHE-1664580) and Cornell University is gratefully acknowledged, as is the U.S. Dept of Energy, Office of Basic Energy Sciences for partial support of this research (TRC, DE-FG02-03ER15387). NSF support for the CCB NMR facility (NSF-MRI CHE-1531632) is appreciated, as is technical aid from Ivan Keresztes. We thank Emil B. Lobkovsky for solving the crystal structure of **3**.

REFERENCES

(1) (b) Lyaskovskyy, V.; de Bruin, B. Redox Non-innocent Ligands: Versatile New Tools to Control Catalytic Reactions. *ACS Catal.* **2012**, 2, 270−129. (c) te Grotenhuis, C.; de Bruin, B. Radical-type

DOI: 10.1021/acs.organomet.8b00930
Organometallics 2019, 38, 1502−1515

Reactions Controlled by Cobalt: From Carbene Radical Reactivity to the Catalytic Intermediacy of Reactive *o*-Quinodimethanes. *Synlett* **2018**, *29*, 2238−2250. (a) Dzik, W. I.; de Bruin, B. Open-shell organometallics: reactivity at the ligand. *Organomet. Chem.* **2011**, *37*, 46.

(2) (a) Chirila, A.; van Vliet, K. M.; Paul, N. D.; de Bruin, B. [Co(MeTAA)] Metalloradical Catalytic Route to Ketenes via Carbonylation of Carbene Radicals. *Eur. J. Inorg. Chem.* **2018**, *2018*, 2251−2258. (b) Chirila, A.; Brands, M. B.; de Bruin, B. Mechanistic investigations into the cyclopropanation of electron deficient alkenes with ethyl diazoacetate using [Co(MeTAA)]. *J. Catal.* **2018**, *361*, 347−360.

(3) (a) Wen, X.; Wang, Y.; Zhang, X. P. Enantioselective radical process for synthesis of chiral indolines by metalloradical alkylation of diverse C(sp^3)-H bonds. *Chem. Sci.* **2018**, *9*, 5082−5086. (b) Wang, Y.; Wen, X.; Cui, X.; Zhang, X. P. Enantioselective Radical Cyclization for Construction of 5-Membered Ring Structures by Metalloradical C-H Alkylation. *J. Am. Chem. Soc.* **2018**, *140*, 4792−4796. (c) Jiang, H. L.; Lang, K.; Lu, H. J.; Wojtas, L.; Zhang, X. P. Asymmetric Radical Bicyclization of Allyl Azidoformates via Cobalt(II)-Based Metalloradical Catalysis. *J. Am. Chem. Soc.* **2017**, *139*, 9164−9167. (d) Wang, Y.; Wen, X.; Cui, X.; Wojtas, L.; Zhang, X. P. Asymmetric Radical Cyclopropanation of Alkenes with In Situ Generated Donor-Substituted Diazo Reagents via Co(II)-Based Metalloradical Catalysis. *J. Am. Chem. Soc.* **2017**, *139*, 1049−1052.

(4) (a) Dzik, W. I.; Xu, X.; Zhang, X. P.; Reek, J. N. H.; de Bruin, B. 'Carbene Radicals' in Co-II(por)-Catalyzed Olefin Cyclopropanation. *J. Am. Chem. Soc.* **2010**, *132*, 10891−10902. (b) Dzik, W. I.; Zhang, X. P.; de Bruin, B. Redox Noninnocence of Carbene Ligands: Carbene Radicals in (Catalytic) C-C Bond Formation. *Inorg. Chem.* **2011**, *50*, 9896−9903.

(5) (a) Russell, S. K.; Hoyt, J. M.; Bart, S. C.; Milsmann, C.; Stieber, S. C. E.; Semproni, S. P.; DeBeer, S.; Chirik, P. J. Synthesis, electronic structure and reactivity of bis(imino)pyridine iron carbene complexes: evidence for a carbene radical. *Chem. Sci.* **2014**, *5*, 1168−1174. (b) Russell, S. K.; Lobkovsky, E.; Chirik, P. J. N-N Bond Cleavage in Diazoalkanes by a Bis(imino)pyridine Iron Complex. *J. Am. Chem. Soc.* **2009**, *131*, 36−37.

(6) Frazier, B. A.; Wolczanski, P. T.; Keresztes, I.; DeBeer, S.; Lobkovsky, E. B.; Pierpont, A. W.; Cundari, T. R. Synthetic Approaches to $(smif)_2$Ti (smif = 1,3-di-(2-pyridyl)-2-azaallyl) Reveal Redox Non-Innocence and C-C Bond-Formation. *Inorg. Chem.* **2012**, *51*, 8177−8186.

(7) (a) Frazier, B. A.; Williams, V. A.; Wolczanski, P. T.; Bart, S.; Meyer, K.; Cundari, T. R.; Lobkovsky, E. B. C-C Bond Formation and Related Reactions at the CNC Backbone in (smif)FeX (smif = 1,3-di-(2-pyridyl)-2-azaallyl): Dimerizations, 3 + 2 Cyclization, and Nucleophilic Attack; Transfer Hydrogenations and Alkyne Trimerization (X = $N(TMS)_2$ dpma (di-(2-pyridyl-methyl)-amide)). *Inorg. Chem.* **2013**, *52*, 3295−3312. (b) Frazier, B. A.; Wolczanski, P. T.; Lobkovsky, E. B.; Cundari, T. R. Unusual Electronic Properties of the Dipyridylazaallyl LIgand: Characterization of $(smif)_2M^n$ (n = 0, M = Fe, Co, Ni; n = + 1, M = Co; smif = $\{(2\text{-py})CH\}_2N$) and $[(TMS)_2NFe]_2(smif)_2$. *J. Am. Chem. Soc.* **2009**, *131*, 3428−3429. (c) Frazier, B. A.; Wolczanski, P. T.; Lobkovsky, E. B. Aryl-Containing Chelates and the Discovery of 1,3-Di-2-pyridyl-2-azaallyl (smif) via CN Bond Activation: Structures of $\{\kappa\text{-}C,N,N^{py}_2\text{-}(2\text{-pyridylmethyl})_2N(CH_2(4\text{-}^tBu\text{-phenyl-2-yl}))\}$FeBr and $(smif)CrN(TMS)_2$. *Inorg. Chem.* **2009**, *48*, 11576−11585. (d) Frazier, B. A.; Bartholomew, E. R.; Wolczanski, P. T.; DeBeer, S.; Santiago-Berrios, M.; Abruña, H. D.; Lobkovsky, E. B.; Bart, S. C.; Mossin, S.; Meyer, K.; Cundari, T. R. Synthesis and Characterization of $(smif)_2M^n$ (n = 0, M = V, Cr, Mn, Fe, Co, Ni, Ru; n = + 1, M = Cr, Mn, Co, Rh, Ir; smif = 1,3-di-(2-pyridyl)-2-azaallyl). *Inorg. Chem.* **2011**, *50*, 12414−12436.

(8) Morris, W. D.; Wolczanski, P. T.; Sutter, J.; Meyer, K.; Cundari, T. R.; Lobkovsky, E. B. Iron and Chromium Complexes Containing Tridentate Chelates Based on Nacnac and Imino- and Methyl-Pyridine Components: Triggering C-C(X) Bond Formation. *Inorg. Chem.* **2014**, *53*, 7467−7484.

(9) Volpe, E. C.; Wolczanski, P. T.; Darmon, J. M.; Lobkovsky, E. B. Syntheses and Characterizations of α-Iminopyridine Compounds $(AlkylN = CHpy)_2Fe(L/X_n)$, and an Assessment of Redox Non-Innocence. *Polyhedron* **2013**, *52*, 406−415.

(10) Williams, V. A.; Hulley, E. B.; Wolczanski, P. T.; Lancaster, K. M.; Lobkovsky, E. B. Pushing the limits of redox non-innocence: pseudo square planar $[\{\kappa^4\text{-}Me_2C(CH_2N = CHpy)_2\}Ni]^n$ (n = 2+, 1+, 0, −1, −2) favor Ni(II). *Chem. Sci.* **2013**, *4*, 3636−3648.

(11) Hulley, E. B.; Wolczanski, P. T.; Lobkovsky, E. B. Carbon-carbon Bond Formation from Azaallyl and Imine Couplings About Metal-metal Bonds. *J. Am. Chem. Soc.* **2011**, *133*, 18058−18061.

(12) Hulley, E. B.; Williams, V. A.; Morris, W. D.; Wolczanski, P. T.; Hernández-Burgos, K.; Lobkovsky, E. B.; Cundari, T. R. Disparate Reactivity from Isomeric $\{Me_2C(CH_2N = CHpy)_2\}$ and $\{Me_2C(CH = NCH_2\ py)_2\}$ Chelates in Iron Complexation. *Polyhedron* **2014**, *84*, 182−191.

(13) (a) Lindley, B. M.; Wolczanski, P. T.; Cundari, T. R.; Lobkovsky, E. B. 1st Row Transition Metal and Lithium Pyridine-ene-amide Complexes Exhibiting N- and C-Isomers and Ligand-based Activation of Benzylic C-H Bonds. *Organometallics* **2015**, *34*, 4656−4688. (b) Jacobs, B. P.; Wolczanski, P. T.; Lobkovsky, E. B. Oxidatively Triggered Carbon-carbon Bond Formation in Ene-amide Complexes. *Inorg. Chem.* **2016**, *55*, 4223−4232.

(14) Heins, S. P.; Morris, W. D.; Wolczanski, P. T.; Lobkovsky, E. B.; Cundari, T. R. Nitrene Insertion into CC and CH Bonds of Diamide-diimine Ligated Chromium and Iron Complexes. *Angew. Chem., Int. Ed.* **2015**, *54*, 14407−14411.

(15) Heins, S. P.; Wolczanski, P. T.; Cundari, T. R.; MacMillan, S. N. Redox non-innocence permits catalytic nitrene carbonylation by (dadi)Ti═NAd (Ad = adamantyl). *Chem. Sci.* **2017**, *8*, 3410−3418.

(16) Heins, S. P.; Morris, W. D.; Cundari, T. R.; MacMillan, S. N.; Lobkovsky, E. B.; Livezey, N.; Wolczanski, P. T. Complexes of $[(dadi)Ti(L/X)]^m$ that Reveal Redox Non-innocence, and a Stepwise Carbene Insertion into a Carbon-carbon Bond. *Organometallics* **2018**, *37*, 3488−3501.

(17) (a) Ray, K.; Petrenko, T.; Wieghardt, K.; Neese, F. Joint spectroscopic and theoretical investigations of transiton metal complexes involving non-innocent ligands. *Dalton Trans.* **2007**, 1552−1566. (b) Lu, C. C.; Bill, E.; Weyhermüller, T.; Bothe, E.; Wieghardt, K. Wieghardt, Neutral bis(alpha-iminopyridine)metal complexes of the first-row transiton metal ions (Cr, Mn, Fe, Co, Ni, Zn) and their monocationic analogues: Mixed valency involving a redox noninnocent ligand system. K. *J. Am. Chem. Soc.* **2008**, *130*, 3181−3197.

(18) Chirik, P. J. Iron- and Cobalt-Catalyzed Alkene Hydrogenation: Catalysis with Both Redox-Active and Strong Field Ligands. *Acc. Chem. Res.* **2015**, *48*, 1687−1695.

(19) Munhá, R. F.; Zarkesh, R. A.; Heyduk, A. F. Group transfer reactions of d^0 transition metal complexes: redox-active ligands provide a mechanism for expanded reactivity. *Dalton Trans.* **2013**, *42*, 3751−3766.

(20) Caulton, K. G. Systematics and Future Projections Concerning Redox-Noninnocent Amide/Imine Ligands. *Eur. J. Inorg. Chem.* **2012**, *2012*, 435−443.

(21) Allen, F. H.; Kennard, O.; Watson, D. G.; Brammer, L.; Orpen, A. G.; Taylor, R. Tables of Bond Lengths Determined by X-ray and Neutron Diffraction. 1. Bond Lengths in Organic Compounds. *J. Chem. Soc., Perkin Trans. 2* **1987**, S1−S19.

(22) Addison, A. W.; Rao, T. N.; Reedijk, J.; van Rijn, J.; Verschoor, G. C. Synthesis, structure, and spectroscopic properties of copper(II) compounds containing nitrogen−sulphur donor ligands; the crystal and molecular structure of aqua[1,7-bis(*N*-methylbenzimidazol-2′-yl)-2,6-dithiaheptane]copper(II) perchlorate. *J. Chem. Soc., Dalton Trans.* **1984**, 1349−1356.

(23) Olsen, J. The CASSCF method: A perspective and commentary. *Int. J. Quantum Chem.* **2011**, *111*, 3267−3272.

DOI: 10.1021/acs.organomet.8b00930
Organometallics 2019, 38, 1502−1515

(24) Stevens, W. J.; Krauss, M.; Basch, H.; Jasien, P. G. Relativistic compact effective potentials and efficient, shared-exponent basis sets for the third-, fourth-, and fifth-row atoms. *Can. J. Chem.* **1992**, *70*, 612−630.
(25) (a) Cahill, R.; Cookson, R. C.; Crabb, T. A. Geminal Coupling Contants in Methylene Groups-II. *Tetrahedron* **1969**, *25*, 4681−4709. (b) Reich, H. J. 5-HMR-4 Geminal Proton-Proton Couplings ($^2J_{H-H}$), 2018. https://www.chem.wisc.edu/areas/reich/nmr/05-hmr-04-2j.htm (accessed on 1/12/19).
(26) Tsurugi, H.; Saito, T.; Tanahashi, H.; Arnold, J.; Mashima, K. Carbon Radical Generation by d^0 Tantalum Complexes with α-Diimine Ligands through Ligand-Centered Redox Processes. *J. Am. Chem. Soc.* **2011**, *133*, 18673−18683.
(27) (a) Kochi, J. K. *Organometallic Mechanisms and Catalysis*; Academic Press: New York, 1978. (b) Hartwig, J. F. *Organotransition Metal Chemistry*; University Science Books: Mill Valley, CA, 2010.
(28) Parshall, G. W.; Mrowca, J. σ-Aryl and -Alkyl Derivarives of Transition Metals. *Adv. Organomet. Chem.* **1969**, *7*, 157−209.
(29) (a) Williams, G. M.; Gell, K. I.; Schwartz, J. Competitive Oxidation Processes in the Reaction between (Dicyclopentadienyl)-zirconium Bis(phosphine) Complexes and Alkyl Halides. *J. Am. Chem. Soc.* **1980**, *102*, 3660−3662. (b) Williams, G. M.; Schwartz, J. Direct Observation of Metal-Centered Radicals in an Oxidative Addition Reaction. *J. Am. Chem. Soc.* **1982**, *104*, 1122−1124.
(30) (a) Monaghan, P. K.; Puddephatt, R. J. Oxidative Addition of Alkyl Halides in the Presence of Alkenes and the Rate of Addition of an Alkyl Radical to a Platinum(II) Complex. *Organometallics* **1986**, *5*, 439−442. (b) Ferguson, G.; Monaghan, P. K.; Parvez, M.; Puddephatt, R. J. Alkylperoxoplatinum(IV) Complexes Formed by Oxidative Addition of Alkyl Halides in the Presence of Oxygen: The Mechanism of Reaction and the Structure of *trans*-Iodo-(isopropylperoxo)dimethyl(1,10-phenanthroline)-platinum(IV). *Organometallics* **1985**, *4*, 1669−1674. (c) Hill, R. H.; Puddephatt, R. J. A Mechnanistic Study of the Photochemically Initiated Oxidative Addition of Isopropyl Iodide to Dimethyl(1,10-phenanthroline)-platinum(II). *J. Am. Chem. Soc.* **1985**, *107*, 1218−1225. (d) Monaghan, P. K.; Puddephatt, R. Reactivity and mechanism in the oxidative addition of iodoalkanes and di-iodoalkanes to a dimethylplatinum(II) complex. *J. Chem. Soc., Dalton Trans.* **1988**, 595−599.
(31) Hall, T. L.; Lappert, M. F.; Lednor, P. W. Mechanistic Studies of Some Oxidative-addition Reactions: Free-radical Pathways in the Pt^0-RX, Pt^0-PhBr, and Pt^{II}-R'SO_2X Reactions (R = Alkyl, R' = Aryl, X = Halide) and in the Related Rhodium(I) or Iridium(I) Systems. *J. Chem. Soc., Dalton Trans.* **1980**, 1448−1456.
(32) Tejel, C.; Ciriano, M. A.; Edwards, A. J.; Lahoz, F. J.; Oro, L. A. Oxidative-Addition of Organic Monochloro Derivatives to Dinuclear Rhodium Complexes: Mechanistic Considerations. *Organometallics* **2000**, *19*, 4968−4976.
(33) Kramer, A. V.; Labinger, J. A.; Bradley, J. S.; Osborn, J. A. Mechanistic Studies of Oxidative Addition to Low-Valent Metal Complexes. III. Mechanism of Formation of Platinum to Carbon Bonds. *J. Am. Chem. Soc.* **1974**, *96*, 7145−7147.
(34) Boisvert, L.; Denney, M. C.; Hanson, S. K.; Goldberg, K. I. Insertion of Molecular Oxygen into a Palladium(II) Methyl Bond: A Radical Chain Mechanism Involving Palladium(III) Intermediates. *J. Am. Chem. Soc.* **2009**, *131*, 15802−15814.
(35) Weix, D. J. Methods and Mechanisms for Cross-Electrophile Coupling of Csp^2 Halides with Alkyl Electrophiles. *Acc. Chem. Res.* **2015**, *48*, 1767−1775.
(36) Griller, D.; Ingold, K. U. Free-radical Clocks. *Acc. Chem. Res.* **1980**, *13*, 317−3223.
(37) Newcomb, M. Competition Methods and Scales for Alkyl Radical Reaction Kinetics. *Tetrahedron* **1993**, *49*, 1151−1176.
(38) Wigley, D. E.; Karlin, K. D. Organoimido Complexes of the Transition-metals. *Prog. Inorg. Chem.* **2007**, *42*, 239−482.
(39) Nugent, W. A.; Mayer, J. M. *Metal−Ligand Multiple Bonds*; Wiley-Interscience: New York, 1988.
(40) Luo, H.-R. *Handbook of Bond Dissociation Energies of Organic Compounds*; CRC Press: New York, 2003.
(41) (a) Bordwell, F. G. Equilibrium Acidities in Dimethyl Sulfoxide Solution. *Acc. Chem. Res.* **1988**, *21*, 456−4763. (b) Reich, H. J. Bordwell pK_a Table (Acidity in DMSO), 2012. https://www.chem.wisc.edu/areas/reich/pkatable/ (accessed on 1/12/19).

DOI: 10.1021/acs.organomet.8b00930
Organometallics 2019, 38, 1502−1515